JOURNAL OF NEMATOLOGY

Research Paper | DOI: 10.2478/jofnem-2024-0026

e2024-1 | Vol. 56

First Report and Molecular Variability of *Belonolaimus longicaudatus* Associated with Turfgrass in Maryland

Benjamin Waldo[1,*], Andrea Skantar[1], Zafar Handoo[1], Shiguang Li[1], Alemayehu Habteweld[1] and Fereshteh Shahoveisi[2]

[1]Mycology and Nematology Genetic Diversity and Biology Laboratory, USDA, ARS, Northeast Area, Beltsville, MD 20705

[2]Department of Plant Sciences and Landscape Architecture, University of Maryland, College Park, MD 20742

*E-mail: Benjamin.Waldo@usda.gov

This paper was edited by Adrienne M. Gorny.

Received for publication September 25, 2023.

Abstract

Turfgrass is a crop used extensively in athletic fields and golf courses in Maryland. A soil sample collected in July 2023 from an athletic field in Baltimore County, Maryland, part of a turfgrass nematode survey, contained *Belonolaimus longicaudatus*. In the southeastern United States, *B. longicaudatus* is an economically important pathogen of warm season turfgrass. The density was four individuals/100 cm^3 of soil, and no visual symptoms were observed in the bermudagrass field. Morphological features and morphometrics of males and females were consistent with *B. longicaudatus* and placed the Maryland population in a subclade that was geographically represented by populations from north and west Florida, Texas, and South Carolina. Sequencing of the internal transcribed spacer region ITS1 and ITS2 and 28S large ribosomal subunit D2-23 expansion region confirmed the species' identity. Phylogenetic trees and parsimony network analysis placed the Maryland isolate in a large grouping of *B. longicaudatus* populations including those from Alabama, Delaware, Florida, Indiana, Mississippi, South Carolina, and Texas. To our knowledge, this is the first report of *B. longicaudatus* in Maryland.

Keywords

28S rRNA, *Belonolaimus longicaudatus*, detection, ITS rRNA, Maryland, molecular, morphology, morphometrics, phylogenetics, statistical parsimony, sting nematode, taxonomy, turfgrass

Belonolaimus longicaudatus is an economically relevant nematode with an extensive host range (Rau, 1958; Riggs, 1982). Although *B. longicaudatus* can be problematic in sandy soils on a range of crops, it is possibly best known for the detrimental impact it has on turfgrass quality (Boyd et al., 1972; Busey et al., 1991; Giblin-Davis et al., 1992; Schwartz et al., 2010; Crow et al., 2013). In the southeastern United States, *B. longicaudatus* is one of the most problematic pathogens of bermudagrass (*Cynodon dactylon*), a warm season turfgrass commonly used in athletic fields and golf courses (Riggs, 1982; Crow et al., 2005; Shaver et al., 2017). *Belonolaimus longicaudatus* has a lengthy stylet that is capable of penetrating deep into the root cortex and severely injuring the meristems of roots and root hairs. Impaired root uptake of water can increase host susceptibility to environmental stress, and yellowing and declining turfgrass can be associated with heavy feeding pressure (Crow and Han, 2005). Within the United States, *B. longicaudatus* has been reported in Alabama, Arkansas, California, Connecticut, Delaware, Florida, Georgia, Indiana, Kansas, Louisiana, Mississippi, Missouri, Nebraska, New Jersey, North Carolina, Oklahoma, South Carolina, Texas, and Virginia, but has yet to be reported in Maryland (CABI, 2021).

In addition to morphological and pathogenicity studies, several molecular investigations using internal transcribed spacer (ITS) and/or 28S rRNA genes have identified population groupings associated with geographic location, including the so-called

type "A" associated with the Atlantic coastal plains, namely, western and central Florida (Gozel et al., 2006), Delaware (Handoo et al., 2010), and Georgia and North Carolina (Han et al., 2006), with presumed introduction of this type in California (Mundo-Ocampo et al., 1994; Cherry et al., 1997); type "B" limited to south Florida; type "C" from northwest Florida; and other types found to be associated with *B. gracilis, B. euthychilus,* or *B. maluceroi* (Cid del Prado Vera and Subbotin, 2012).

The objective of this project was to characterize *Belonolaimus* nematodes detected in turfgrass soil from Maryland using morphological and molecular tools. The results of this work represent the first record of the sting nematode, *B. longicaudatus,* in the state of Maryland.

Materials and Methods

Sample collection and morphological study

During a turfgrass nematode survey, a composite soil sample was collected from an asymptomatic athletic field with "North Bridge" bermudagrass in Baltimore County, MD in July 2023. The sample was processed at the U.S. Department of Agriculture, Agricultural Research Service, Mycology and Nematology Genetic Diversity and Biology Laboratory in Beltsville, MD. Nematodes were extracted from soil using sugar flotation and centrifugation (Jenkins, 1964). Adult and juvenile *Belonolaimus* were initially observed with an inverted microscope at a density of four individuals/100 cm^3 of soil. Morphometric measurements were performed on 10 females and 10 males.

Molecular study

Molecular confirmation was performed by sequencing two ribosomal markers that have robust representation in GenBank. The ribosomal ITS regions ITS1 and ITS2 and the D2-D3 expansion regions of 28S large subunit rRNA were obtained from five females. ITS-CL-F2 (5′-ATTACGTCCCTGCCCTTTGTA-3′)/ D2AR (5′-ACTTTCCCTCACGGTACTTGT-3′) and 28S-CL-F1 (5′-ACTTTCCCTCACGGTACTTGT-3′)/ D3B (5′-TCGGAAGGAACCAGCTACTA-3′) primer sets were used to obtain comprehensive coverage of target loci with cycling conditions as described previously (Carta and Li, 2018; 2019). Forward and reverse sequences for each marker were aligned and assembled into a consensus sequence and subsequently queried using the BLASTn tool from the National Center of Biotechnology Institute (ncbi.nlm.nih.gov) to determine species identity. Newly obtained sequences were submitted to GenBank under the accession numbers OR520202 and OR520203 for ITS and OR520268 and OR520269 for 28S.

Separate ITS and 28S rRNA sequence alignments were constructed with *B. longicaudatus* populations from GenBank in MAFFT within Geneious and trimmed with GBlocks to eliminate poorly aligned regions. Outgroups included *Tylenchus annulatus* (EF030983) for ITS and *T. leviterminalis* (KJ461550) for 28S. In order to align data from GenBank that include different parts of the ITS rRNA gene, 18S-ITS1-5.8S sequences and outgroup taxa were added to the longer 18S-ITS1-5.8S-ITS2-28S alignment as described in Mundo-Ocampo et al. (2017) by using the MAFFT-add option on the MAFFT v7.0 server (http://mafft.cbrc.jp/alignment/server) (Katoh and Standley, 2013). For both ITS and 28S alignments, the model of base substitution was selected using jModelTest 2.1.2 (Darriba et al., 2012). The Akaike-supported model, a general time-reversible model including among-site rate heterogeneity and estimates of invariant sites (GTR + G + I), was used in further analysis. Bayesian analyses were run using the MrBayes CIPRES plugin within Geneious. Bayesian inference (BI) analysis for each gene included a random starting tree and was run with four chains for 2 x 10^6 generations. Two runs were performed for each analysis. Trees were sampled every 1,000th generation, with 25% of the results discarded as burnin. The remaining samples were used to generate a 50% majority rule consensus tree. Posterior probabilities (PP) are shown on appropriate clades. The alignments minus outgroup taxa and outlier *B. longicaudatus* sequences were also used to construct phylogenetic networks via statistical parsimony (SP) using the program PopART (http://popart.otago.ac.nz) (Leigh and Bryant, 2015).

Results

Measurements and description

Morphometrics and characteristics of adult specimens were consistent with *B. longicaudatus* (Tables 1,2; Fig. 1). Bodies of females and males were slender and cylindrical, lip region was rounded and offset, stylet was slim and long with rounded stylet knobs, and the esophagus overlapped the intestine. Females were didelphic with hemispherical tails (Fig. 1A). Males possessed curved spicules and a bursa that enveloped the tail end (Fig. 1B).

Table 1. Morphometrics of *Belonolaimus longicaudatus* females collected from bermudagrass in Baltimore County, Maryland compared with the original species description and females of two *B. longicaudatus* subclades from Habteweld et al. (2021).

Characteristics[a]	MD population (*n* = 10)	*B. longicaudatus* (*n* = 22) (Rau, 1958)	Subclade IIIA (*n* = 20) (Habteweld, 2021)	Subclade IIIB (*n* = 20) (Habteweld, 2021)
L	2.5 ± 0.2 (2.2-2.8)	2.2 (2.0-2.6)	-	-
a	65 ± 5 (58-73)	65.4 (55.7-74.9)	-	-
b	8 ± 1 (7-9)	8.4 (7.3-9.9)		
c	20 ± 2 (15-23)	16.1 (14.5-18.0)	-	-
V%	50 ± 1 (49-52)	50 (46-54)	-	-
Esophagus length	277 ± 7.39 (263-287)	-	257 ± 22 (199-311)	269 ± 26 (211-316)
Excretory pore distance	257 ± 9.12 (236-267)	215 (184-233)	210 ± 18 (144-233)	226 ± 26 (171-264)
Lip length	9.1 ± 0.83 (8-10)	17.8 (16.8-18.8)	9.6 ± 1.1 (6.7-12.2)	10.3 ± 1.2 (7.8-12.9)
Stylet length	122 ± 5 (110-126)	118 (100-133)	118 ± 7 (102-129)	126 ± 8 (99-142)
Stylet cone	88 ± 6 (75-95)	93 (84-102)		
Stylet shaft	34 ± 2 (30-35)	34 (28-39)		
Stylet knob width	5.9 ± 0.32 (5.5-6.5)	-	5.4 ± 0.5 (4.5-6.4)	5.7 ± 0.5 (5.0-6.7)
Tail length	128 ± 14 (114-150)	140 (177-163)		
Tail/body width ratio	4 ± 0 (4-5)	4.4 (3.5-5.0)	-	-
Tail width	32 ± 3 (28-38)	-	-	-
Tail integument thickness	6.9 ± 0.91 (5.5-8.0)	-	6.7 ± 1.2 (4.8-10.1)	7.2 ± 0.9 (5.4-9.1)
Stylet length/Tail length ratio	1.0 ± 0.1 (0.82-1.1)	0.81 (0.68-1.0)	0.87 ± 0.07 (0.72-1.0)	0.94 ± 0.08 (0.78-1.2)

[a]All characteristics are measured in micrometers, except for L, which is measured in millimeters. Morphometrics are presented as mean ± standard deviation (range).

The MD population morphometric means were compared to morphometric means of subclades IIIB and IIIA from Habteweld et al. (2021) due to interpopulation variation that exists in morphology and morphometrics in *B. longicaudatus*. MD morphometric means were closest in value to the IIIB subclade means in stylet knob width, excretory pore distance from anterior, esophagus length, and stylet/tail length ratio, relative to the IIIA subclade (Table 1). Excretory pore distance from the anterior of the MD population was the only measurement that did not have overlapping ranges with the IIIA subclade selected characteristics. The morphometrics of subclades IIIB and IIIA presented in Table 2 were found to be statistically different between the two subclades by Habteweld et al. (2021). The subclades were defined by geographical region with subclade IIIB composed of populations from north and west Florida, Texas, and South Carolina and subclade IIIA made up of south Florida populations.

Molecular characterization

For 28S rRNA, sequences of 721 bp were obtained from five females, of which four were identical and one differed at 2 bp from the others. BLASTn of the single representative was 100% identical to *B. longicaudatus* sequences obtained from Florida (peanut; KF963100), Texas (soil; MZ045460), and several others; the other sequence representing four individuals was 99.7% identical to the same accessions (0.3%, 2-bp differences). For ITS rRNA,

Table 2. Morphometrics of *Belonolaimus longicaudatus* males collected from bermudagrass in Baltimore County, Maryland compared with the original species description.

Characteristics[a]	MD population (*n* = 10)	*B. longicaudatus* (*n* = 22) (Rau, 1958)
L	1.9 ± 0.95 (1.8-2.1)	1.8 (1.6-2.1)
a	57 ± 3 (52-62)	64 (55-74)
b	7 ± 1 (6-8)	7.5 (7.0-8.1)
c	15 ± 1 (13-17)	15 (13-17)
Stylet length	113 ± 4 (108-120)	120 (111-132)
Stylet cone	82 ± 5 (76-90)	-
Stylet shaft	31 ± 2 (28-33)	-
Tail length	131 ± 8 (120-145)	-
Spicule length	42 ± 4 (35-45)	43 (0.76-0.97)
Gubernaculum length	18 ± 2 (15-20)	17 (15-18)

[a]All characteristics are measured in micrometers, except for L, which is measured in millimeters. Morphometrics are presented as mean ± standard deviation (range).

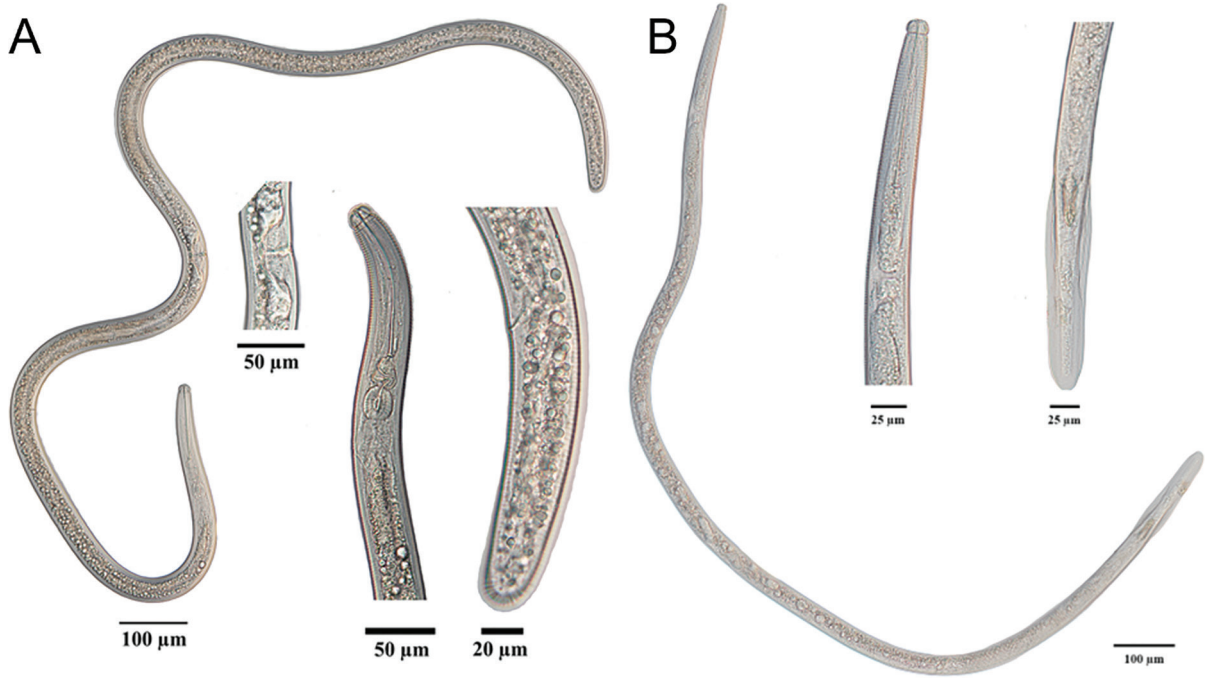

Figure 1. Photomicrographs of *Belonolaimus longicaudatus* female (A) and male (B) specimens.

sequences 867 bp in length were obtained from two females, with 3-bp differences between them. BLASTn showed 99.4% identity (0.6%, 3- to 5-bp differences) with *B. longicaudatus* sequences obtained from Delaware (soybean; GQ896549) and Florida (citrus; DQ672364) and high similarity to several others.

Phylogenetic relationships

Newly obtained 28S rRNA sequences were aligned with all known *Belonolaimus* spp. sequences from GenBank, with *Tylenchorhynchus leviterminalis* (KJ461550) used as the outgroup. The 28S phylogenetic tree inferred by Bayesian analysis (Fig. 2)

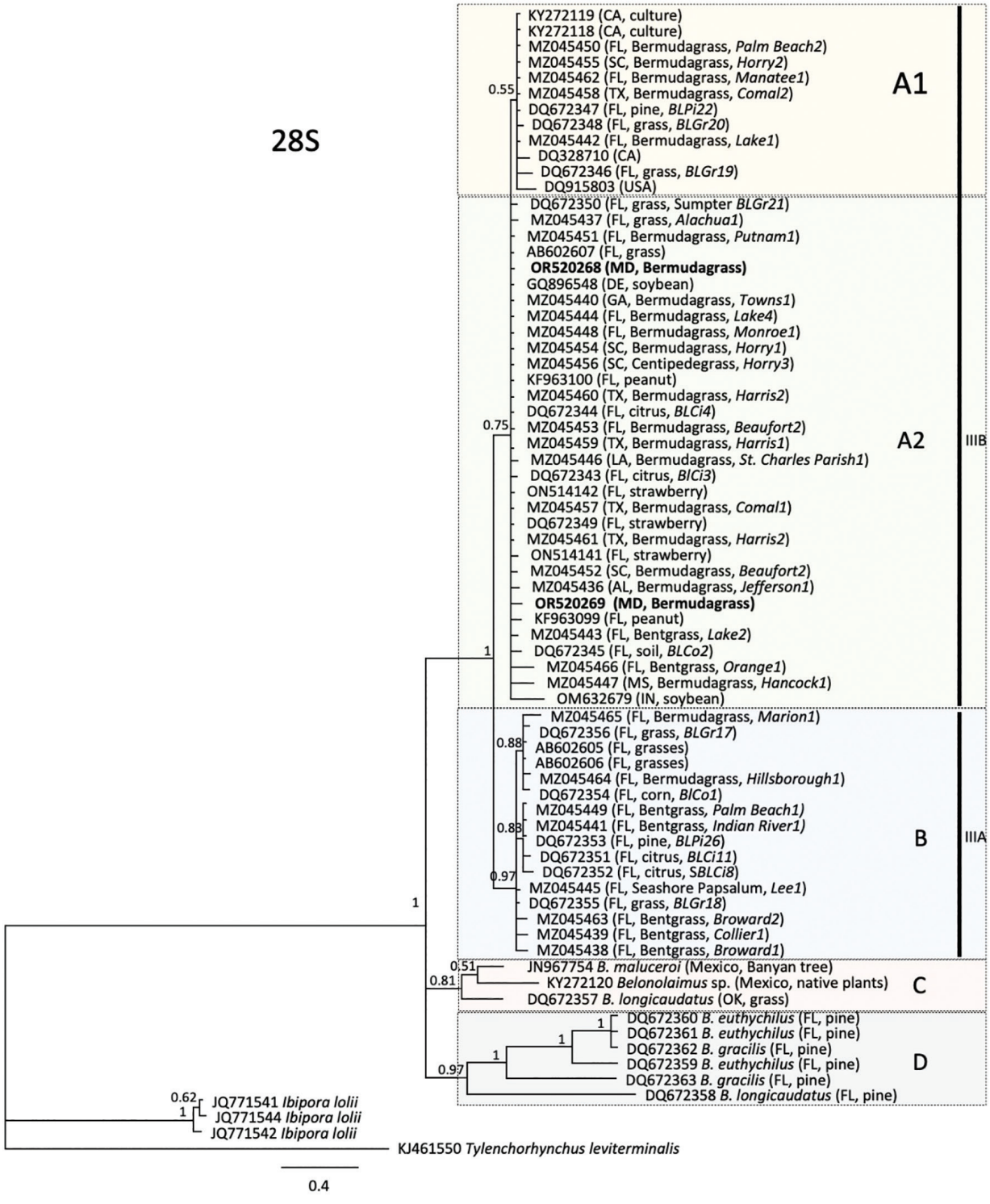

Figure 2. Molecular phylogeny of *Belonolaimus* species as inferred from Bayesian inference of the 28S D2-D3 expansion region of ribosomal RNA under the GTR + I + G model of nucleotide substitution. The 50% majority rule consensus tree from Bayesian inference is presented. Posterior probabilities are given for appropriate clades. Newly obtained sequences are in bold. Shaded regions A to D indicate corresponding groupings in Figure 4 of Mundo-Ocampo et al. (2017). Roman numerals indicate groupings shown in Figure 1 of Habteweld et al. (2021).

showed that *B. longicaudatus* 28S sequences formed a single clade, with the Maryland population included in the largest subclade (Group A2) along with others from Florida (various hosts), Alabama and Georgia (bermudagrass), Delaware and Indiana (soybean), South Carolina (bermudagrass and centipedegrass), Mississippi (bermudagrass), and Texas (bermudagrass). Group A1 contained populations from Florida, California, South Carolina, and Texas. Group B was placed as a sister clade to Group A and was composed of south Florida populations from bermudagrass, bentgrass, seashore paspalum, citrus, corn, turf plugs, or soil. Outlier sequences DQ672357 (from Oklahoma turfgrass) appeared in Group C with *B. maluceroi* from Mexico (banyan tree), and DQ672358 (from Florida pine) appeared in a polyphyletic clade Group D with *B. euthychilus* and *B. gracilis* populations from Florida pine. Support for the separation of subclades A1 and A2 was low; however, the separation between Group A1/A2 and Group B was maximally supported (PP = 1).

Newly obtained ITS rRNA sequences were aligned with *Belonolaimus* spp. sequences from GenBank, with *T. annulatus* (EF030983) as the outgroup. Some of the *B. longicaudatus* data from GenBank included only ITS1; thus, following the MAFFT-add alignment strategy employed by Mundo-Ocampo et al. (2017) was effective in preserving the main alignment while allowing distant sequences and outgroups to be included without introducing unnecessary gaps. To simplify the comparison with previous phylogenetic trees, we not only followed the clade designations of Mundo-Ocampo et al. (2017) with some modifications, but also referred to the Roman numeral clade assignments (IIIA and IIIB) in Figures 3 and 4 of Habteweld et al. (2021). The phylogenetic tree (Fig. 3) inferred by BI produced three major groupings and placed the Maryland population of *B. longicaudatus* within the largest subclade (Group A2; PP = 1) that included populations from Delaware and Indiana (found on soybean); Florida (from a variety of hosts); North Carolina (corn), Louisiana, Texas, and South Carolina (bermudagrass); Georgia (cotton or bentgrass); and Barbados (grasses). Group A1 populations came mainly from Florida and Texas, but also included others from California, Mississippi, and South Carolina. Together, A1 and A2 correspond to Group A as previously described (Mundo-Ocampo et al., 2017). Group B was dominated by Florida populations and one population from Texas. There was strong support for the separation of subclades A1 and A2 (PP = 0.91) and for the separation of Group A from Group B (PP = 0.96). There was also strong support for Group C that included *B. maluceroi* (isolated from Banyan tree in Mexico), an unnamed *Belonolaimus* sp. (KY272122 and KY272123), and apparent outlier populations *B. longicaudatus* from Texas (grass; DQ494800), Nebraska (corn; DQ494801), and South Carolina (U89696). The most divergent *B. longicaudatus* population was from Florida pine (DQ672384), appearing basal to clade D, which included *B. gracilis* and *B. euthychilus*.

Statistical parsimony was applied to the sequence alignments to study the haplotype networks among populations of *B. longicaudatus.* The network for 28S sequences of *B. longicaudatus* is shown in Figure 4. The size of the circles at node points is proportional to the number of sequences that share a haplotype, and geographic locations are indicated by color. For 28S, three main haplotype groupings consistent with the 28S MB tree were observed. Group A1 contained 10 haplotypes, Group A2 contained 8 haplotypes, and Group B contained 9 haplotypes. The Maryland isolate appeared in Group A2 and shared the most dominant haplotype with isolates from Florida, Alabama, Delaware, Georgia, Indiana, South Carolina, and Texas. Group A2 had haplotypes from Florida, California, Mississippi, South Carolina, and Texas. Group B was dominated by south Florida populations. Two outliers, DQ672357 from Oklahoma (grass) and DQ672358 from Florida (pine), were distantly separated from Group B.

Sequences from the ITS parsimony network are shown in Figure 5. GenBank datasets that included only ITS1 were omitted from this analysis. Three main population groupings consistent with the ITS MB tree emerged from the analysis. For ITS, there were only a few haplotypes shared by multiple populations; for the most part, each sequence formed its own branch in the network. Group A1 (composed of 15 haplotypes) was further divided into two sub-branches, with one consisting of sequences from Florida, California, and South Carolina, and the other composed of sequences from Florida, Mississippi, and Texas. The second group, A2 (18 haplotypes), included the two Maryland *B. longicaudatus* sequences and others from diverse locations including Delaware, Florida, Georgia, Indiana, Louisiana, South Carolina, Texas, and the island of Barbados. Group A2 contained the most shared haplotypes. One Maryland sequence (OR520202) shared a haplotype with Texas and Florida isolates. Group B (10 haplotypes) was composed entirely of sequences from Florida isolates, similar to the phylogenetic tree.

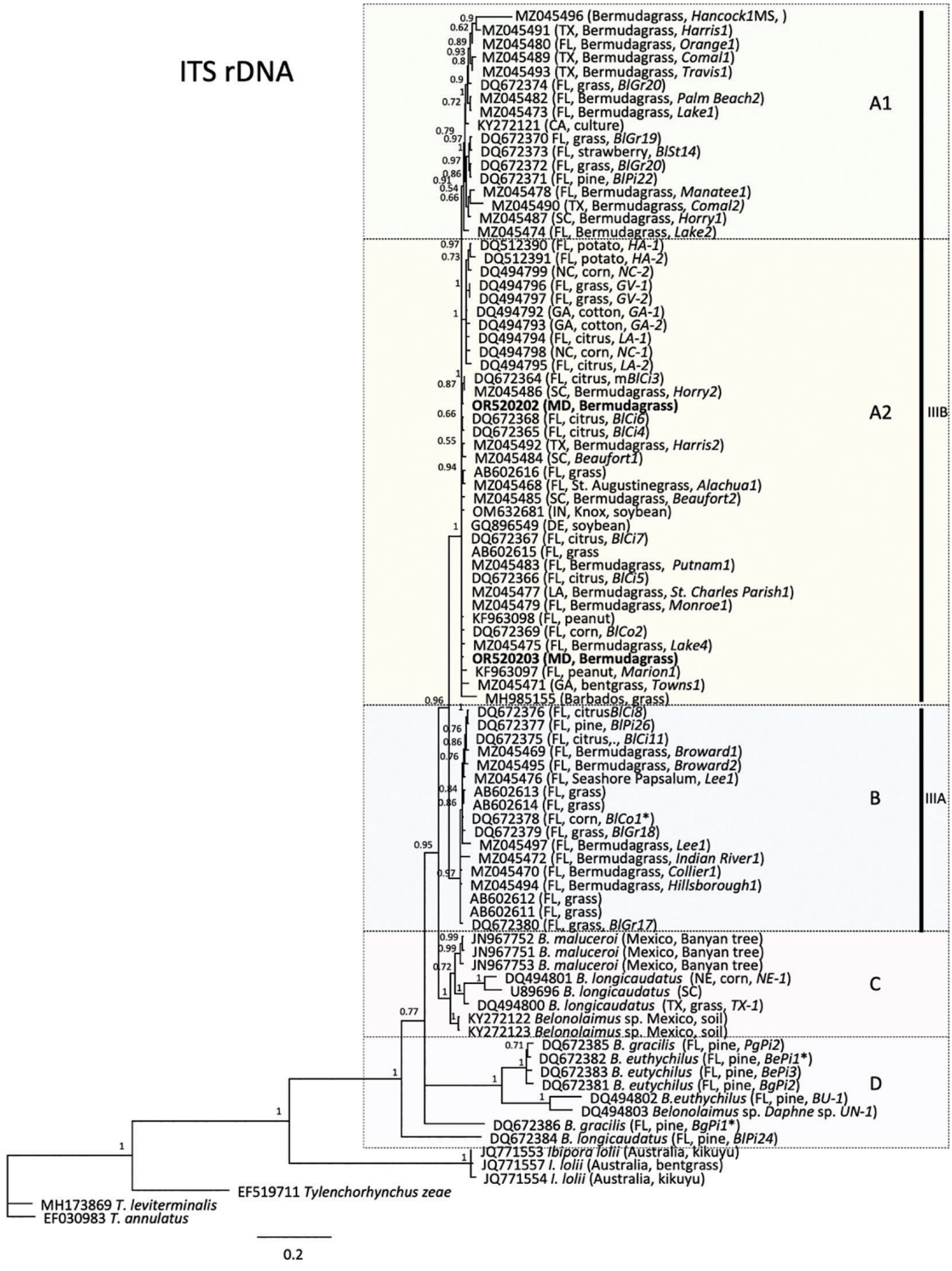

Figure 3. Molecular phylogeny of *Belonolaimus* species as inferred from Bayesian inference of the ITS1 and ITS2 region of ribosomal RNA under the GTR + I + G model of nucleotide substitution. The 50% majority rule consensus tree from Bayesian inference is presented. Posterior probabilities are given for appropriate clades. Newly obtained sequences are in bold. Shaded regions A to D indicate corresponding groupings in Figure 5 of Mundo-Ocampo et al. (2017). Roman numerals indicate groupings shown in Figure 2 of Habteweld et al. (2021). Asterisks indicate topotype populations.

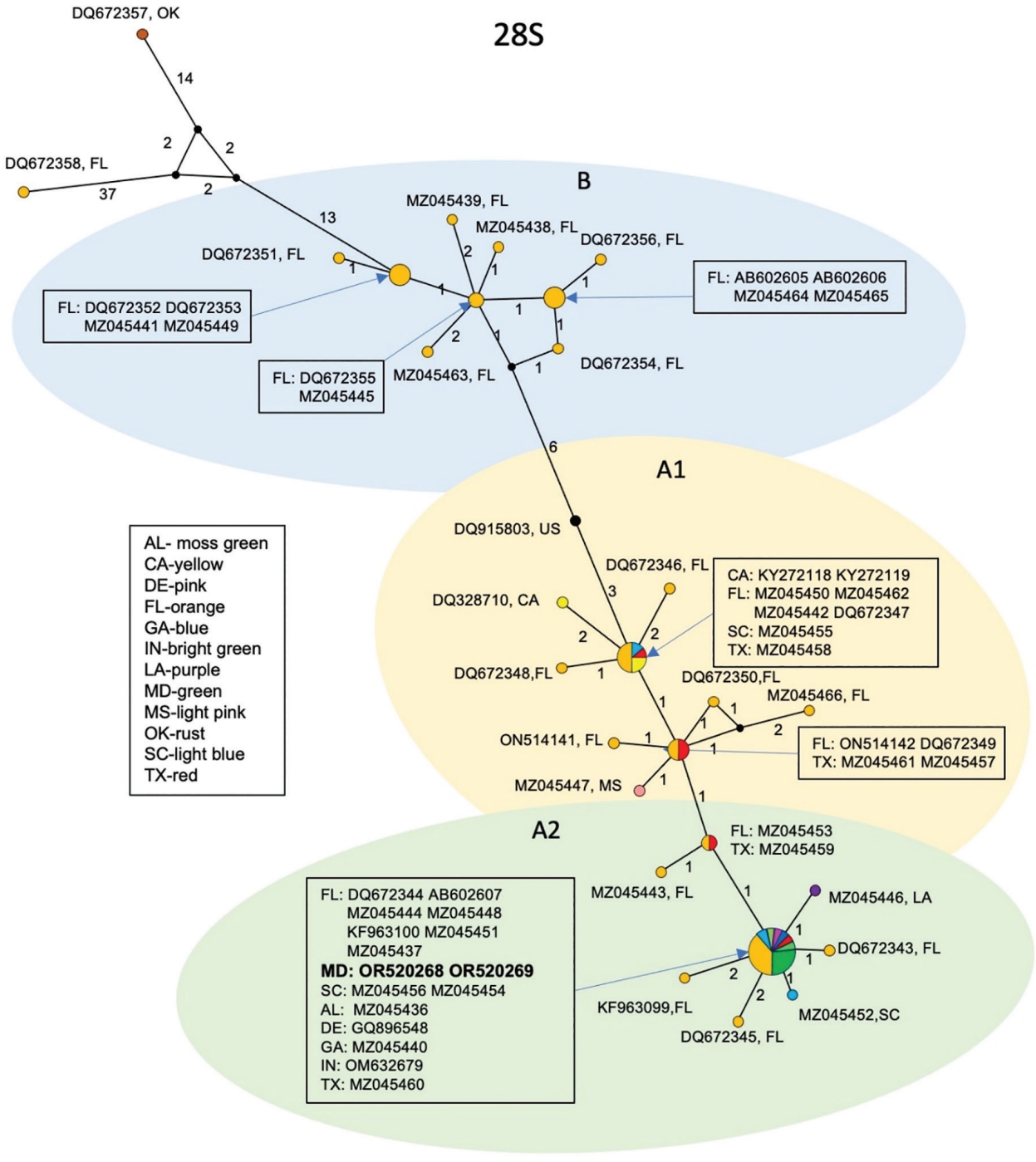

Figure 4. 28S rRNA statistical parsimony network. The sequences of each species are marked by different color circles as indicated in the key. Circles divided into sections represent sequences of each species with the same haplotype, and their size is proportional to the number of these sequences in the samples. Numbers of nucleotide differences between the sequences are indicated on lines connecting the pies. Small black dots represent missing haplotypes. New sequences are indicated in bold font. Color shaded regions A1, A2, and B correspond to groupings in the 28S phylogenetic tree.

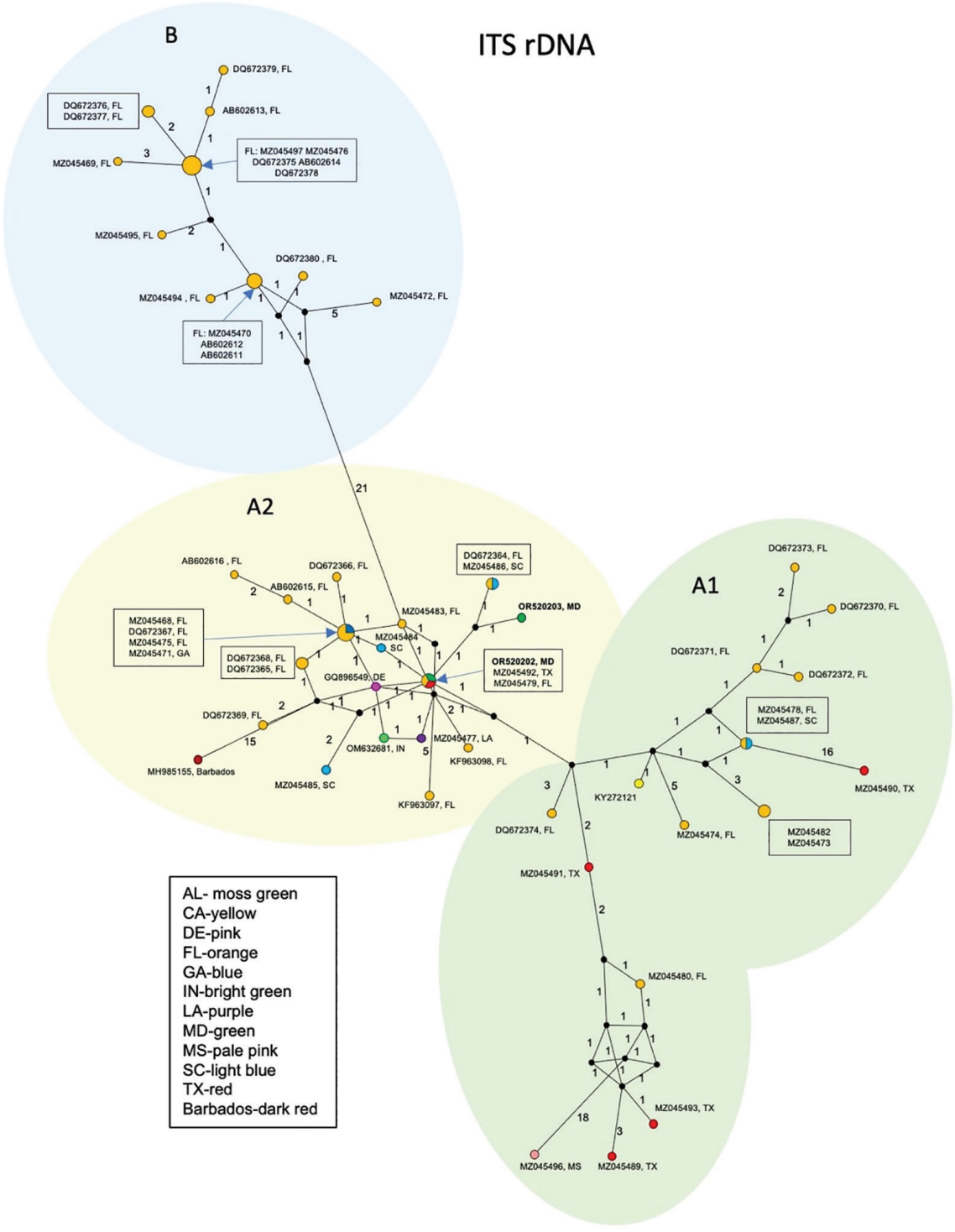

Figure 5. ITS statistical parsimony network. The sequences of each species are marked by different color circles as indicated in the key. Pies (circles) represent sequences of each species with the same haplotype, and their size is proportional to the number of these sequences in the samples. Numbers of nucleotide differences between the sequences are indicated on lines connecting the circles. Small black dots represent missing haplotypes. New sequences are indicated in bold font. Color shaded regions A1, A2, and B correspond to groupings in the ITS phylogenetic tree.

Discussion

This study confirmed the identification of *B. longicaudatus* from turfgrass soil on an asymptomatic athletic field in Baltimore County, Maryland using morphological and molecular means. Morphological features of the Maryland population characteristic of *B. longicaudatus* include having an offset lip region, a stylet longer than 100 µm, and tail length > stylet length with a few exceptions, and the morphometric characteristics were in the range reported for *B. longicaudatus* (Rau, 1958; 1961). The mean values for stylet knob width (5.9 vs. 5.7 µm), excretory pore distance from anterior end (257 vs. 226 µm), esophagus length (277 vs. 269 µm), stylet/tail ratio (1.0 vs. 0.94 µm), and tail integument (6.9 vs. 7.2 µm) of the MD population were closer to the mean values reported for populations in subclade IIIB than in subclade IIIA (Habteweld et al., 2021). Our finding was in line with the previous studies that showed intra-population variations in morphology and morphometrics in *B. longicaudatus* (Robbins and Hirschmann, 1974; Gozel et al., 2006).

Molecular characterization also confirmed identification of the Maryland isolate as *B. longicaudatus* and placed it in context with other known populations of *Belonolaimus* spp. through analysis of 28S and ITS rRNA using phylogenetic methods and SP networks. Assembly of *Belonolaimus* spp. 28S and ITS sequences known to date allowed for comparisons among datasets from previous studies (Gozel et al., 2006; Han et al., 2006; Cid del Prado Vera and Subbotin, 2012; Kutsuwa et al., 2015; Mundo-Ocampo et al., 2017; Habteweld et al., 2021).

The main structure of the phylogenetic trees for ITS1, ITS2, and 28S gave the same general topology as with previous studies, although the different clade names and choices of taxa were not consistent across various studies. Clade A as designated in Mundo-Ocampo et al. (2017) was split into A1 and A2 in our 28S and ITS trees. Although the branch lengths in the trees are very short, this separation becomes apparent in the SP networks; thus, the phylogenetic trees were annotated to match these groups. This corresponds to Clade III in Habteweld et al. (2021). Clade B from the current study corresponds to Clade B from Mundo-Ocampo et al. (2017) with strong supported branches in both ITS and 28S trees (Figs. 2,3). This group corresponds to Group IIIA in Habteweld et al. (2021), who, along with Gozel et al. (2006), described these populations from south Florida and one from north central Florida.

Previous analysis by Han et al. (2006) demonstrated variation in the length of the amplified ITS1 region in the Nebraska isolate (DQ494801) and the Texas isolate (DQ494800), which had a 40-bp deletion from the middle of ITS1. In our ITS tree, the Nebraska and Texas sequences appeared in Group C, along with *B. maluceroi* and an unnamed isolate from Mexico. It is not clear if the outcome would be different had the full ITS1 and ITS2 been available, but this result agreed with those of Cid del Prado Vera and Subbotin (2012) and Mundo-Ocampo et al. (2017).

In Habteweld et al. (2021), three ITS sequences, KF963098 (peanut, Florida), GQ896549 (soybean, Delaware), and AB602614 (grasses, Florida), were grouped in a clade together with *B. maluceroi* in what they designated Clade I (our Group C). Our results disagree with this finding, placing the former two sequences instead in Group A2 (Habteweld's IIIB) and placing the latter AB602614 in Group B (equivalent to their IIIA). Our results agree with those of Mundo-Ocampo et al. (2017), as their dataset and ours contain all three sequences in question and are placed similarly. Cid del Prado Vera and Subbotin (2012) included only the Delaware sequence and not the other two, but our results also agree with theirs. Likewise, the ITS tree from Kutsuwa et al. (2015) places KF963098 or GQ896549 in the equivalent of our Group A2 and not close to *B. maluceroi.* The reason for this discrepancy in Habteweld et al. (2021) is unclear, but it is possible that differences in alignment or tree-building methods caused those results. Other studies and ours have indeed shown that some *B. longicaudatus* populations do group with *B. maluceroi* (DQ494801, Nebraska, corn; U89696, South Carolina; DQ494800, Texas, bermudagrass), and DQ672384 (Florida, pine) does appear outside the main *B. longicaudatus* clade, closer to *B. gracilis*, showing support for a species complex (Cid del Prado and Subbotin, 2012; Kutsuwa et al., 2015; Mundo-Ocampo et al., 2017). However, KF963098, GQ596549, and AB602614 are not among those that give support to the apparent polyphyly of *Belonolaimus.* Moreover, the positions of these populations in the 28S trees (sequences KF963099, GQ896548, and AB602605) are consistent with the ITS placements in our analysis and others' (Mundo-Ocampo et al, 2017).

The topology of Groups C and D in our 28S and ITS trees are somewhat different from that of Mundo-Ocampo et al. (2017), although internally, the sequences within the clades agree. The 28S tree places *B. longicaudatus* (DQ672358, Florida, pine)

with the polyphyletic *B. euthychilus/B. gracilis* group with strong support (PP = 0.97) and the Oklahoma population close to *B. maluceroi* (PP = 0.81). Likewise, both ITS trees group *B. longicaudatus* from Nebraska (DQ494801), Texas (DQ494800), South Carolina (U89696), and the unnamed Sinaloa, Mexico isolate (KY272122) with *B. maluceroi*, and group the North Carolina population from *Daphne* sp. (DQ494803) and one from Florida pine (DQ672384) together with the *B. gracilis/B. euthychilus* group.

The molecular analysis places the Maryland isolate of *B. longicaudatus* within a large, diverse clade in terms of geography and host, and trees resulting from combining several existing datasets together give support for *B. longicaudatus* as a polyphyletic species complex. The SP network analysis is very useful for visualizing relationships among sequence haplotypes from the different populations in a manner that typical phylogenetic trees do not always show.

Acknowledgments

Alemayehu Habteweld was supported in part by an appointment to the Research Participation Program at the Mycology and Nematology Genetic Diversity and Biology Laboratory, U.S. Department of Agriculture (USDA), Agricultural Research Service (ARS), Northeast Area, Beltsville, MD, administered by the Oak Ridge Institute for Science and Education through an inter-agency agreement between the U.S. Department of Energy and USDA-ARS. The authors would like to thank Bryan Filkins for participating in the turfgrass nematode survey and permitting the authors to collect soil samples. Mention of trade names or commercial products in this publication is solely for the purpose of providing specific information and does not imply recommendation or endorsement by the USDA. USDA is an equal opportunity provider and employer.

Literature Cited

Boyd, F. T., Schroder, V. N., and Perry, V. G. 1972. Interaction of nematodes and soil temperature on growth of three tropical grasses. Agronomy Journal 64:497-500.

Busey, P., Giblin-Davis, R. M., Riger, C. W., and Zaenker, E. I. 1991. Susceptibility of diploid St. Augustinegrasses to *Belonolaimus longicaudatus*. Journal of Nematology 23:604-610.

CABI. 2021. *Belonolaimus longicaudatus* (sting nematode). In: CABI Compendium. Wallingford, UK: CAB International. Nov. 2021. https://www.cabidigitallibrary.org/doi/10.1079/cabicompendium.8892.

Carta, L. K., and Li, S. 2018. Improved 18S small subunit rRNA primers for problematic nematode amplification. Journal of Nematology 50:533-542. doi: 10.21307/jofnem-2018-051

Carta, L. K., and Li, S. 2019. PCR amplification of a long rRNA segment with one primer pair in agriculturally important nematodes. Journal of Nematology 51:1-8. doi: 10.21307/jofnem-2019-026

Cherry, T., Szalanski, A. L., Todd, T. C., and Powers, T. O. 1997. The internal transcribed spacer region of *Belonolaimus* (Nemata: Belonolaimidae). Journal of Nematology 29:23-29.

Cid del Prado Vera, I., and Subbotin, S. A. 2012. *Belonolaimus maluceroi* sp. n. (Tylenchida: Belonolaimidae) from a tropical forest in Mexico and key to the species of *Belonolaimus*. Nematropica 42:201-210.

Crow, W. T., and Han, H. 2005. Sting nematode. The Plant Health Instructor. doi: 10.1094/PHI-I-2005-1208-01

Crow, W. T., Lickfeldt, D. W., and Unruh, J. B., 2005. Management of sting nematode (*Belonolaimus longicaudatus*) on bermudagrass putting greens with 1, 3-dichloropropene. International Turfgrass Society Research Journal 10:734-741.

Crow, W. T., Luc, J. E., Sekora, N. S., and Pang, W. 2013. Interaction between *Belonolaimus longicaudatus* and *Helicotylenchus pseudorobustus* on bermudagrass and seashore paspalum hosts. Journal of Nematology 45:17-20.

Darriba, D., Taboada, G. L., Doallo, R., and Posada, D. 2012. jModelTest 2: more models, new heuristics and parallel computing. Nature Methods 9:772. doi: 10.1038/nmeth.2109

Giblin-Davis, R. M., Cisar, J. L., Bilz, F. G., and Williams, K. E. 1992. Host status of different bermudagrasses (*Cynodon* spp.) for the sting nematode, *Belonolaimus longicaudatus*. Journal of Nematology 24:749-756.

Gozel, U., Adams, B. J., Nguyen, K. B., Inserra, R. N., Giblin-Davis, R. M., and Duncan, L. W. 2006. A phylogeny of *Belonolaimus* populations in Florida inferred from DNA sequences. Nematropica 36:55-171.

Habteweld, A. F., Mendes, M. L., Inserra, R. N., and Crow, W. T. 2021. Phylogenetic relationships of *Belonolaimus longicaudatus* populations associated with turfgrasses in the southeastern USA. Nematropica 51:41-55.

Han, H-R., Jeyaprakash, A., Weingartner, D. P., and Dickson, D. W. 2006. Morphological and molecular biological characterization of *Belonolaimus longicaudatus*. Nematropica 36:37-52.

Handoo, Z. A., Skantar, A. M., and Mulrooney, R. P. 2010. First report of the sting nematode *Belonolaimus longicaudatus* on soybeans in Delaware. Plant Disease 94:133-133. doi: 10.1094/PDIS-94-1-0133B

Katoh, K., and Standley, D. M. 2013. MAFFT multiple sequence alignment software version 7: Improvements in performance and usability. Molecular Biology and Evolution 30:772-780. doi: 10.1093/molbev/mst010

Kutsuwa, K., Dickson, D. W., Brito, J. A., Jeyaprakash, A., and Drew A. 2015. *Belonolaimus longicaudatus*: An emerging pathogen of peanut in Florida. Journal of Nematology 47:87-96.

Leigh, J. W., and Bryant, D. 2015. PopART: Full-feature software for haplotype network construction. Methods in Ecology and Evolution 6:1110-1116. doi: 10.1111/2041-210X.12410

Mundo-Ocampo, M., Baldwin, J. G., Pereira, T. J., Camacho-Baez, J. R., Armenta-Bojorquez, A. D., Camacho-Haro, M., and Becker, J. O. 2017. Occurrence of *Belonolaimus* in Sinaloa, Northwestern Mexico: A new report on distribution and host range. Journal of Nematology 49:103-113. doi: 10.21307/jofnem-2017-050.

Mundo-Ocampo, M., Becker, J. O., and Baldwin, J. G. 1994. Occurrence of Belonolaimus longicaudatus on Bermudagrass in the Coachella Valley. Plant Disease 78:529.

Rau, G. J. 1958. A New Species of Sting Nematode. Proceedings of the Helminthological Society of Washington 25:95-98.

Rau, G. J. 1961. Amended descriptions of Belonolaimus gracilis Steiner, 1949 and B. longicaudatus Rau, 1958 (Nematoda: Tylenchida). Proceedings of the Helminthological Society of Washington 28:198-200.

Riggs, R. D. 1982. Nematology in the southern region of the United States. Southern Cooperative Series Bulletin 276. Fayetteville, AK: Arkansas Agricultural Experiment Station.

Robbins, R. T., and Hirschmann, H. 1974. Variation among populations of *Belonolaimus longicaudatus*. Journal of Nematology 6:87-94.

Schwartz, B. M., Kenworthy, K. E., Crow, W. T., Ferrell, J. A., Miller, G. L., and Quesenberry, K. H. 2010. Variable responses of zoysiagrass genotypes to the sting nematode. Crop Science 50:723-729. doi: 10.2135/cropsci2008.11.0672

Shaver, B. R., Agudelo, P., and Martin, S. B. 2017. Damage functions for sting nematode (*Belonolaimus longicaudatus*) on bermudagrass turf. International Turfgrass Society Research Journal 13:517-523. doi: 10.2134/itsrj2016.06.0478